Biochemical and Biophysical Research Communications 447 (2014) 178–183

Contents lists available at ScienceDirect

Biochemical and Biophysical Research Communications

journal homepage: www.elsevier.com/locate/ybbrc

Crystal structure of the catalytic domain of PigE: A transaminase involved in the biosynthesis of 2-methyl-3-*n*-amyl-pyrrole (MAP) from *Serratia* sp. FS14

Xiangdi Lou [a,1], Tingting Ran [a,1], Ning Han [a], Yanyan Gao [a], Jianhua He [b], Lin Tang [c], Dongqing Xu [a,*], Weiwu Wang [a,*]

[a] Key Laboratory of Agricultural and Environmental Microbiology, Ministry of Agriculture, College of Life Sciences, Nanjing Agricultural University, 210095 Nanjing, China
[b] Shanghai Institute of Applied Physics, Chinese Academy of Sciences, Shanghai, China
[c] Shanghai Institutes for Biological Sciences, Chinese Academy of Sciences, Shanghai, China

ARTICLE INFO

Article history:
Received 21 March 2014
Available online 2 April 2014

Keywords:
PigE
Crystal structure
MAP
Prodigiosin

ABSTRACT

Prodigiosin, a tripyrrole red pigment synthesized by *Serratia* and some other microbes through a bifurcated biosynthesis pathway, MBC (4-methoxy-2,2′-bipyrrole-5-carbaldehyde) and MAP (2-methyl-3-*n*-amyl-pyrrole) are synthesized separately and then condensed by PigC to form prodigiosin. MAP is synthesized sequentially by PigD, PigE and PigB. PigE catalyzes the transamination of an amino group to the aldehyde group of 3-acetyloctanal, resulting in an aminoketone, which spontaneously cyclizes to form H_2MAP. Here we report the crystal structure of the catalytic domain of PigE which involved in the biosynthesis of prodigiosin precursor MAP for the first time to a resolution of 2.3 Å with a homodimer in the asymmetric unit. The monomer of PigE catalytic domain is composed of three domains with PLP as cofactor: a small N-terminal domain connecting the catalytic domain with the front part of PigE, a large PLP-binding domain and a C-terminal domain. The residues from both monomers build the PLP binding site at the interface of the dimer which resembles the other PLP-dependent enzymes. Structural comparison of PigE with *Thermus thermophilus* AcOAT showed a higher hydrophobic and smaller active site of PigE, these differences may be the reason for substrate specificity.

1. Introduction

Prodigiosins, a kind of red-pigmented secondary metabolites with linear tripyrrole structure, are produced by marine bacteria [1], actinomycetes (e.g. *Streptomyces coelicolor* A3(2)) [2] and some species of *Serratia* [3] only in the later stages of bacterial growth. Although the physiological role of prodiginines in their host microorganisms remains unclear [4], many studies *in vitro* showed that prodigiosins have anti-bacterial, anti-fungal, anti-protozoal/anti-malarial, anti-cancer, anti-stroke, anti-proliferation and trypanolytic activities [5]. Prodigiosin and its synthetic derivatives also have been shown to have potent and specific immunosuppressive activity [6].

Biosynthesis gene clusters from different microorganisms were cloned and sequenced. A gene cluster with *pigA-N* for the prodigiosin production was first identified in the *Serratia* sp. ATCC 39006, with the knock-out mutations of each biosynthetic gene sequentially in this cluster, analysis of the intermediates accumulating in each mutant and with genetic complementation studies, a bifurcated pathway for the prodigiosin production was determined: PigI, PigG, PigA, PigJ, PigH, PigM, PigF and PigN were assigned for the biosynthesis of the one terminal products 4-methoxy-2,2-bipyrrole-5-carboxyaldehyde (MBC) and PigD, PigE and PigB are involved in the biosynthesis of monopyrrole, 2-methyl-3-*n*-amyl-pyrrole (MAP), MBC and MAP are then condensed to form the final product prodigiosin by the PigC [1,7–9]. The biosynthesis pathway of MBC in *Serratia* is essentially the same as that in *S. coelicolor* A3(2), but the synthesis pathways of MAP are completely different, in fact, none of the proteins involved in the biosynthesis of MAP in *Serratia* have close homologs in the *red* cluster of *S. coelicolor* A3(2) which synthesize the prodigionines in the *S. coelicolor* [10]. Among the three enzymes in the MAP pathway: PigD has homology with thiamine pyrophosphate (TPP)-requiring enzymes, and is proposed to transfer a two-carbon fragment from pyruvate (with the loss of a CO_2) to 2-octenal, yielding 3-acetyloctanal; PigE, an aminotransferase, then transfers an amino group to the aldehyde group of

* Corresponding authors.
E-mail addresses: dqxu@njau.edu.cn (D. Xu), wwwang@njau.edu.cn (W. Wang).
[1] These authors contribute equally.

http://dx.doi.org/10.1016/j.bbrc.2014.03.125
0006-291X/

3-acetyloctanal, resulting in an aminoketone, which spontaneously cyclizes to form H2MAP; and finally PigB oxidizes H2MAP to yield MAP [10].

The aminotransferases catalyze the transfer of amino groups to keto compounds by a ping-pong bi–bi reaction mechanism involving two half-reactions [11], using pyridoxal 5′-phosphate (PLP) as a cofactor, is the key enzyme in the biosynthetic pathway of amino acids [12], so these enzymes are principally in the catabolism and the anabolism of amino acids and amino acid-derived metabolites. Aminotransferases are widely distributed in nature, and catalyze a large variety of reactions. Based on the solved structure, they all use PLP as a cofactor at their active center, so aminotransferases belong to the PLP-dependent enzymes. Aminotransferases have been divided into four subgroups, PigE is a putative aminotransferase, and can be classified into subgroup II [13]. It shares similarity with a putative aminotransferase from *S. coelicolor* A3(2). PigE is also one of the only two *pig* genes that do not have homologs in the *red* cluster of *S. coelicolor* [7].

To elucidate the mechanism of the aminotransferase PigE, in this study, we first cloned and expressed the full-length gene of PigE from *Serratia* sp. FS14 [14] in *Escherichia coli*, and crystallized PigE by the vapor diffusion method. Here, we report the crystal structure of the catalytic domain of PigE at 2.3 Å for the first time and the structural comparison between PigE and other amino transferases.

2. Materials and methods

2.1. Gene cloning, protein expression and purification

The DNA encoding full-length PigE was amplified through PCR method with the chromosomal DNA of *Serratia* sp. FS14 as template. PCR was carried out with *Pfu* DNA polymerase (Thermo) with the following primers 5′-atatcatATGAAATTCGGATTCATCGCTC and 5′-gcgtaagcttGTCTAAAAAGGTGGAGAGTTCCTCG corresponding to the 5′ and 3′ ends of the gene, respectively. The restriction sites, *Nde*I and *Hin*dIII, in the primers are underlined, respectively. The PCR product was then digested with *Nde*I and *Hin*dIII and then cloned into the pET24b digested with the same restriction enzymes to create the expression plasmid pET24b-pigE. This plasmid containing the full-length PigE gene with C-terminal His_6-tagged was verified by restriction-enzyme digestion and DNA sequencing. The verified plasmid was then transformed into *E. coli* C43 (DE3) for induction.

A single fresh colony of *E. coli* C43 (DE3) with the pET24b-pigE was cultured at 310 K and grown to OD_{600} as 1.0. The cells were then induced with 0.5 mM IPTG and grown for another 4 h at 299 K. The induced cells were collected by centrifugation at 5000 rev min^{-1} (Hitachi Rotor R20A2) for 10 min and the cell pellet was then resuspended in binding buffer containing of 50 mM K_2HPO_4/KH_2PO_4 pH 7.6, 300 mM NaCl, 5 mM imidazole and 1 mM PMSF just before sonication. After the removal of unbroken cells and insoluble materials by centrifugation for 30 min at 15,000 rev min^{-1} (Hitachi Rotor R20A2), the target protein was purified by immobilized metal-affinity chromatography (IMAC) on Ni–NTA Superflow (Qiagen). Briefly, the supernatant was loaded onto a 2 ml bed volume Ni–NTA column previously equilibrated with 6 bed volumes of binding buffer. Then the column was washed with binding buffer containing 5, 20, and 50 mM imidazole respectively (six bed volumes each) to wash out the unbound or weakly bound proteins, the target protein was eluted using a stepwise increasement of imidazole in elute buffers with 100 and 250 mM imidazole, respectively.

The His_6-tagged PigE were mainly eluted at 100 mM imidazole. The elute protein was concentrated to approximately 2 ml by centrifugation with an Amicon Ultra-15 filter (Millipore), then PLP and four different L-form amino acids: alanine, serine, proline, methionine were added to the protein sample with the final concentration of 1 mM each. After incubation for 1 h, the sample was concentrated to approximately 1.2 ml by centrifugation, and then loaded onto a Sephacryl S300 (Pharmacia Biotech) column pre-equilibrated with 20 mM HEPES pH 7.5 containing 300 mM NaCl, 10% glycerol. The column was then eluted with 1.2 bed volumes of the same buffer. The elution pattern showed that there were three peaks, which were further analyzed by SDS–PAGE for purity check. Since the first peak appeared at the position of the void volume of the column, and the third small peak with pale yellowish shows no protein bands, suggesting it may be the unbound free PLP. So the second peak containing PigE protein was pooled together and concentrated to 10 mg/ml for the crystallization. The protein concentration was determined from the absorbance at 280 nm, assuming an ε280 of 0.811 for a 1.0 mg/ml protein solution.

2.2. Protein crystallization

Initial crystallization screens were performed using six different screening kits from Hampton Research (HR110, 112, 114, 122, 128 and 144) and four MCSG screening kits (MCSG 1-4T) employing the sitting-drop vapor-diffusion method at 295 K. The initial screen yielded rod-shaped crystals from the following condition: pH6.9, 0.49 M NaH_2PO_4, 0.91 M K_2HPO_4, and thick hexagonal plate crystals from the following condition: 0.1 M Tris:HCl pH 8.5, 1 M $MgSO_4$. Since the hexagonal crystals need a long time to grow to full size (more than two months), we chose the first condition for further optimization. The optimization was carried out by grid screening of the precipitate concentration, the pH of the crystallization condition, different concentrations of the protein sample combined with commercial additive and detergent screens (Hampton Research).

The best crystal suitable for diffraction was obtained by mixing 1 ml 10 mg/ml protein solution with the same amount of reservoir solution and equilibrating against 50 μl reservoir solution (pH 6.9, 0.49 M NaH_2PO_4, 0.91 M K_2HPO_4, 50 mM $MgCl_2$ and 3.2 mM *n*-nonyl-*b*-D-maltoside). The crystal obtained from the initial screen with the condition (0.1 M Tris:HCl pH 8.5, 1 M $MgSO_4$) diffracted also very well.

2.3. Data collection and structure determination

Prior to cryocooling, crystals were looped out from the crystallization drop and sequentially transferred into fresh mother liquor, mother liquor with 5% glycerol, mother liquor with 10% glycerol and mother liquor with 15% glycerol for a few seconds each. After transfer to the final solution, the crystal was flash-cooled in liquid nitrogen. Complete X-ray diffraction data sets were collected at beamline BL17U1 of Shanghai Synchrotron Radiation, Shanghai, People's Republic of China using an ADSC Q315r detector. The best crystal diffracted to 2.3 Å resolution. Each frame was exposed for 1.2 s with a rotation range of 1.0. The data were processed using the XDS package [15]. The structure of PigE was solved by the automatic molecular replacement pipeline Balbes [16] using 1VEF as a starting model. The model was then manually adjusted with the program coot [17]. Structure refinement was carried out using REFMAC5 [18]. PyMol was used to prepare the structure Figures [19]. The data processing and structure refinement statistics are summarized in Table SI.

3. Results

3.1. PigE belongs to the PLP-dependent aspartate aminotransferase superfamily

The PigE protein consists of 853 amino acid residues with a predicted molecular mass of 93.26 KDa, and its encoding gene is located in a *pig* cluster (prodigiosin synthesis gene cluster) transcribed as a polycistronic message RNA. It shares 100% sequence identity with the PigE from *Serratia marcescens* WW4 (NCBI accession number YP 007404923.1). The purified recombinant PigE showed the similar molecular size as the predicted size (Fig. S1A). The BLAST search result revealed that the protein has a putative pyridoxal 5′-phosphate (PLP) binding site and belongs to PLP-dependent aspartate aminotransferase superfamily (fold I). The BLAST search also showed several homologs from *Serratia* species, with sequence identities of 100–85%, have corresponding PLP binding sites. We also found that several homologs from other species, such as *Pseudoalteromonas rubra*, *Janthinobacterium lividum*, *Ralstonia solanacearum*, and *Hahella ganghwensis*, with sequence identities of 80–52%, also contain PLP cofactor binding sites. Sequence analysis showed that the C terminal of PigE (residue 372–853) is the putative catalytic domain, which shares some homology with the PLP-dependent aminotransferase family proteins, but the function for the N-terminal domain (residue 1–371) is unclear.

3.2. Overall structure of PigE

The recombinant full length PigE from *Serratia* sp. FS14 was purified by IMAC and gel filtration and then crystallized in a space group P321, with unit-cell parameters $a = b = 124.1$, $c = 73.6$ Å. The crystal structure of PigE was solved by means of molecular replacement using acetylornithine aminotransferase structure (PDB code, 1VEF, Matsumura et al., unpublished data) as the searching template with the molecular-replacement pipeline Balbes, and the PigE structure was refined to an R work of 23.78% (R free 27.18%) at 2.3 Å resolution. The asymmetric unit of the crystal contains two molecules which forms a dimeric structure. Surprisingly, the final model contains only 481 amino acids, including residues from Ala372 to Asp853, no electron density visible for the fragment from residues Met1 to Ala371. The SDS–PAGE analysis of the PigE crystals after diffraction showed that the recovered protein from the crystal was only about 55 KDa, this implied that the protein degraded during crystallization (Fig. S1B).

The asymmetric unit of the crystal contains a truncated PigE dimer of structurally identical monomers (referred to as monomer A and monomer B, respectively) with the backbone rmsd (root mean square deviation) of 0.46 Å. In the final model, both monomers include the residues from 372 to 853, but no electron density visible for residues from 745 to 765 of chain A and 743 to 765 of chain B, respectively. So this fragment is not included in the final model. The Ramachandran plot shows that 95.1%, 4.5%, and 0.4% of phi/psi angles are in favoured, allowed regions, and disallowed, respectively. The data processing and structure refinement statistics are summarized in Table SI.

In each monomer 40% residues form 18 α-helices and 10% form 13 β-strands. The topology of PigE monomer was shown as Fig. 1. Each monomer contains three domains: a small N-terminal domain (residues 372–451, magenta), a large PLP-binding domain (residues 452–703, blue), and a C-terminal domain (residues 704–853, red). The N-terminal domain consists of three α-helices (α1–3) and a β-sheet made of three antiparallel strands (β1–β3). The large PLP-binding domain consists of a seven-stranded mixed β-sheet (β4–β10) and an eleven α-helices (α4–α14). The C-terminal domain is composed of three β-strands (β11–β13) and four α-helices (α15–α18) including two long helices α17 and α18 formed by residues 774–807 and 835–853, respectively (Fig. 2A). The structure fold of PigE is similar to those of other enzymes of Type I subgroup II family of PLP dependent enzymes.

The two polypeptide chains show an interface characteristic of a tight dimer. The dimer interface is mainly formed by the large PLP-binding domains of the two subunits (Fig. 2B). The dimer interface buries 12663.9 Å^2 or 39% total accessible surface area for each dimmer. The interaction involves fifteen hydrogen bonds and seventeen salt-bridges per dimer.

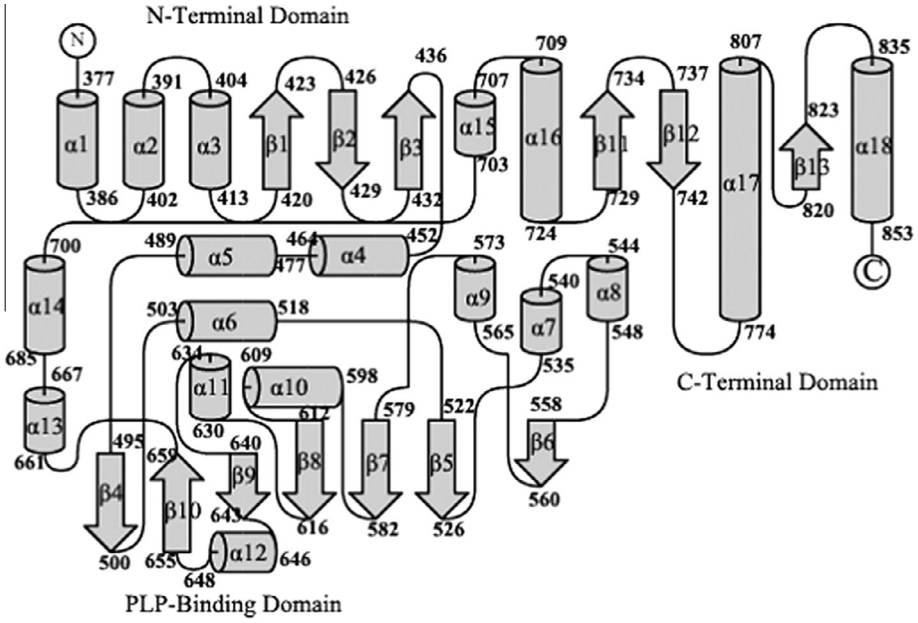

Fig. 1. Topology of secondary structural elements of PigE. The N-terminal domain is formed by a β-sheet β1–3 and three helices α1–3. The large PLP-binding domain is formed by seven β-strand β4–10 and eleven helices α4–14. The C-terminal domain consists of three β-strands β11–13 and four helices α15–18. The diagram was drawn using the program TOPDRAW from CCP4i.

3.3. PLP binding site

The yellowish crystals indicated that PigE protein uses PLP as cofactor. An unambiguous density is observed in the cofactor binding site, and the density is continuous between residues Lys645 and the PLP cofactor, indicating that the expected aldimine had formed between the lysine residue and the PLP. In the asymmetric unit, each monomer binds a PLP as cofactor. Fig. 2B clearly shows the binding of PLP molecules in the cofactor site at the homodimer interface. The cofactors binding site is built up by the residues from both subunits, whereas the active-site cleft is mainly made up of residues from one monomer. One molecule of PLP bound to both subunits in the asymmetric unit. The PLP makes interactions with other residues in the binding site: the side chain OD2 atom of Asp616 forms a charged hydrogen bond with the protonated N1 atom of PLP, stabilizing the protonated N1 to strengthen the electron-withdrawing capacity of PLP; at the same time, the main chain O of Tyr530 formed a weaker hydrogen bond with the protonated N1 atom of PLP; the side chain NE2 of Gln619 is hydrogen-bonded to the O3 atom of PLP, and the negative charge on the O3 atom of PLP stabilizes the protonated form of the imine nitrogen of the external aldimine because they can form an intramolecular hydrogen bond. About the phosphate group of PLP, there are two types coordination: directly interacting with the residues at the binding site by forming hydrogen bond; and through water bridges to link with the residues at the PLP binding site. The O1P atom makes a direct hydrogen bond to the N atom of Gly503, and also through two water molecules to make hydrogen bonds

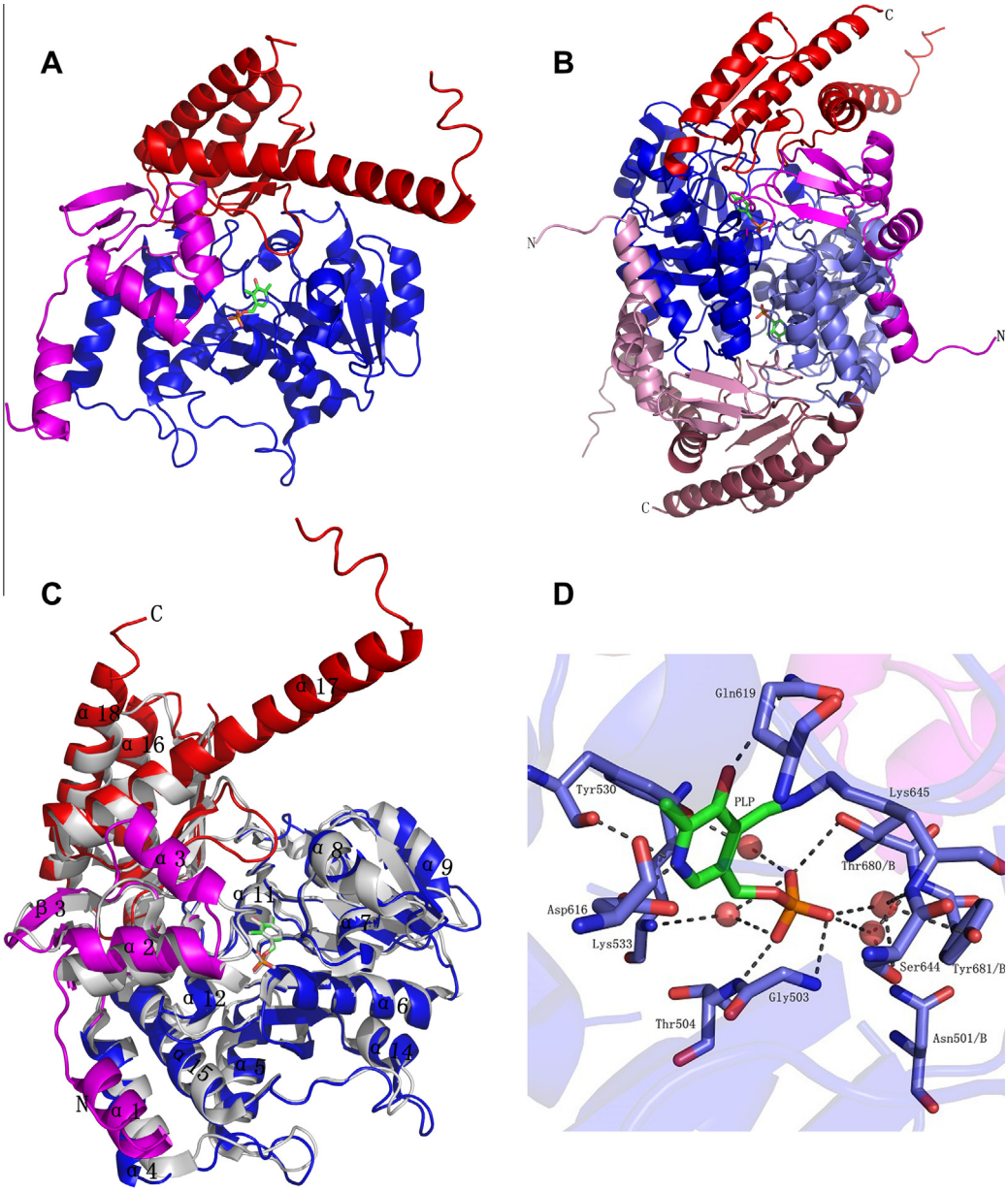

Fig. 2. (A) Three-dimensional structure of a monomeric unit (subunit A) of PigE. Individual domains are colored differently. Magenta: small N-terminal domain; blue: large PLP-binding domain; red: C-terminal domain. PLP is shown as a stick model and the C actoms are colored green. (B) The structure of PigE dimer present in the asymmetric unit. The large interface between the PLP-binding domains (blue) of subunits A and B may be noticed. Two atoms of PLP (C atoms with green) are shown in the PLP-binding domain, respectively. Different domains of subunit B are colored with lighter shade. (C) The comparison of the monomeric unit of PigE to the monomeric unit of 1VEF (tAcOAT), the structure of 1VEF is colored with gray. (D) The hydrogen bonds formed by the residues of PLP binding site and the PLP cofactor. The hydrogen bonds are shown as dotted line and colored with gray30. The cartoon of PigE structure is shown as 80% transparency. The water molecules are shown in spheres and the connecting residues are shown in sticks. (For interpretation of the references to color in this figure legend, the reader is referred to the web version of this article.)

with the side chain OG of Ser644, the main chain N atom of Lys645 from the same chain, the side chain OH and the main chain N atom of Tyr681, and the side chain ND2 of Asn501 from another chain, respectively. The main chain N atom of Thr504 forms hydrogen bond directly with the O2P atom of PLP, at the same time the main chain N atoms of Lys533 through a water molecule connected with the O2P atom of PLP. For the atom O3P, it forms hydrogen bond with the side chain OG1 atom of Thr680 belonging to the other chain. Two waters bridge O3P to the side chain OH atom of Tyr530 and the main chain N atom of Lys533 (Fig. 2D). The hydrogen bond interactions with the atoms O1P, O2P and O3P like a base fixing the bottom of PLP. All other hydrogen bonds formed by residues of PLP binding site and the PLP cofactor like a net firmly catch the PLP cofactor at the binding site.

3.4. Comparison of catalytic domain of PigE structure with other structural homologs

The Dali search [20] retrieved the following proteins as those structurally similar to PigE: acetylornithine/acetyl-lysine aminotransferase (tAcOAT) from *Thermus thermophilus* HB8 (PDB entry 1VEF, Matsumura et al., unpublished data), human ornithine aminotransferase (hOAT, PDB entry 1OAT) [21], gamma-aminobutyrate aminotransferase from *E. coli* (GABA-AT, PDB entry 1SFF) [22], and N-succinylornithine transaminase (AstC) from *E. coli* (AstC, PDB entry 4ADE) [23] with high Z scores. The overall backbone fold of PigE was very similar to these proteins (Table SII).

Structure-based sequence alignment of PigE, tAcOAT (PDB entry 1VEF), hOAT (PDB entry 1OAT) and GABA-AT (PDB entry 1SFF) shows that the lysine forming Schiff base with PLP (marked by ●) and most of the active site residues (marked by ◆ and ▲) are structurally conserved (Fig. S2). PigE superposes with tAcOAT, hOAT, and GABA-AT with rms deviations of 1.5 (for 387 target pairs), 1.8 (for 395 target pairs), 2.1 (for 406 target pairs) Å and shares sequence identities of 35%, 31% and 28%, respectively. Despite their low sequence identity (about 35%), PigE shares virtually the same general folds with tAcOAT. However, there are also some significant differences in the structural comparison with tAcOAT. Of the three domains of PigE, the large PLP-binding domain superposes well with corresponding domains of tAcOAT which only with β6 and β7 longer than corresponding segments of tAcOAT. The N-terminal domain just α2 can be superposed well with tAcOAT, and for the α1, α3 are extra for tAcOAT (Fig. 2C). We concerned that α1 may be the helix linked to the front part of the PigE unresolved structure 1-371aa, but crossing α2 which similar to tAcOAT it is also an α3 supernumerary. Differences on the C-terminal domain are obviously as well. The most straightforward difference is α17 helix which is much longer than the corresponding helix in the C-terminal domain of tAcOAT. The α17 helix of monomer A forms crystal contact with the symmetric molecular of monomer B. Since the α17 helix is sitting at the nearby region of the substrate binding pocket, it may interact with PigD or PigB or both for the efficient substrate exchange during the MAP synthesis. Moreover, between β7 and α10 of PigE structure there is just a loop without two small β-sheets in the tAcOAT corresponding domain. In the PigE structure between α4 and β3 was only a loop, but one small α helix (α2 helix) in tAcOAT structure (Fig. 2C).

PigE was also compared with some other members of the same family of enzymes (ornithine-oxo acid transaminase (Rocd) (Anderson SM et al., unpublished data), 2,2-dialkylglycine decarboxylase (DGD) [24], and glutamate-1-semialdehyde aminomutase (GSA-AT)) [25] with PDB entries 3RUY, 1D7U, and 2GSA, respectively. Superposition of CA atoms of PigE with those of 3RUY, 1D7U, and 2GSA results in rms deviations of 1.6 (383 target pairs), 2.1 (for 401 target pairs), and 2.5 (for 392 target pairs) Å and sequence alignment shows identities of 33%, 29% and 23%, respectively (Table SII).

As is observed for tAcOAT, a deep narrow tunnel extending from the protein surface to the PLP binding site serves as a substrate binding site. The overall substrate binding pocket of PigE is similar when compared with 1WKH and 1WKG (Matsumura et al., unpublished data). However from the structural comparison, we found there are comparable differences between PigE and tAcOAT related to the substrate pocket. The most obvious difference is the hydrophobicity of the binding pocket, in PigE structure more hydrophobic residues present in the substrate accessing tunnel than in tAcOAT (Fig. 3A). The binding pocket size at the entrance and the middle part is somehow smaller than that of tAcOAT due to the stretches of side chains into the binding pocket. But the size of binding pocket is still enough for the substrate 3-acetyloctanal (Fig. 3B).

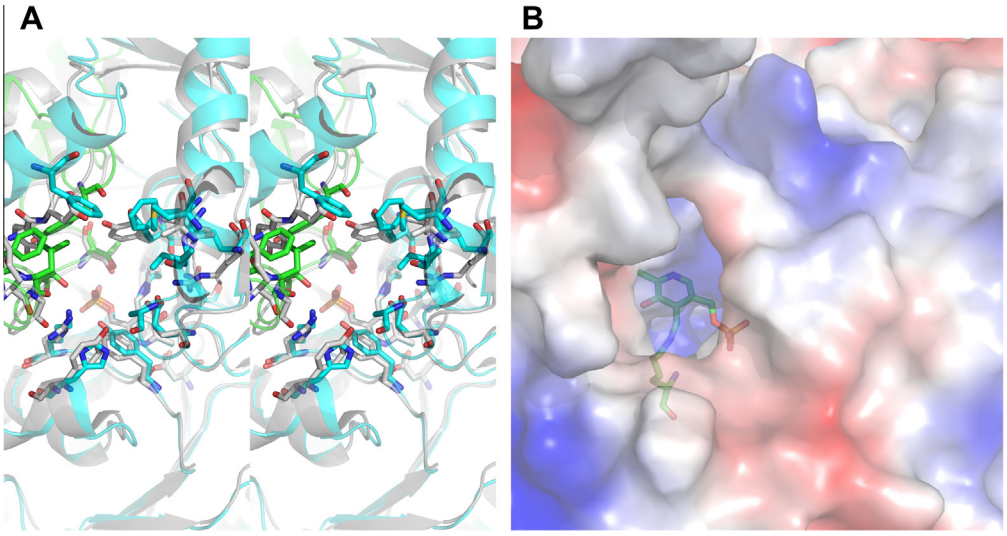

Fig. 3. Substate binding pocket of PigE and its comparison with the substrate binding pocket of tAcOAT. (A) stereo diagrams showing the superimposed active sites of the PigE and tAcOAT (PDB code 1VEF). The backbone of the residues from monomer A, monomer B of PigE are colored cyan and green, the tAcOAT is colored in gray, respectively. (B) The Surface contour image shows the substrate binding pocket of PigE, the Lys645 and PLP sitting in the bottom of the pocket are shown as sticks. (For interpretation of the references to color in this figure legend, the reader is referred to the web version of this article.)

Accession codes

The coordinates for the structure have been deposited in the Protein Data Bank with an ID of (PDB code 4PPM).

Acknowledgments

The authors thank the staff of beamline BL17U at SSRF, Shanghai, People's Republic of China for data collection. This work was supported by a grant from the National Natural Science Foundation of China (31100028) and the Youth Science and Technology Innovation Fund from Nanjing Agricultural University (KJ2013027).

Appendix A. Supplementary data

Supplementary data associated with this article can be found, in the online version, at http://dx.doi.org/10.1016/j.bbrc.2014.03.125.

References

[1] J.S. Lee, Y.S. Kim, S. Park, J. Kim, S.J. Kang, M.H. Lee, S. Ryu, J.M. Choi, T.K. Oh, J.H. Yoon, Exceptional production of both prodigiosin and cycloprodigiosin as major metabolic constituents by a novel marine bacterium, *Zooshikella rubidus* S1–1, Appl. Environ. Microbiol. 77 (2011) 4967–4973.
[2] A.M. Cerdeño, M.J. Bibb, G.L. Challis, Analysis of the prodiginine biosynthesis gene cluster of *Streptomyces coelicolor* A3(2): new mechanisms for chain initiation and termination in modular multienzymes, Chem. Biol. 8 (2001) 817–829.
[3] S.D. Mahlen, *Serratia* infections: from military experiments to current practice, Clin. Microbiol. Rev. 24 (2011) 755–791.
[4] R. Siva, K. Subha, D. Bhakta, A.R. Ghosh, S. Babu, Characterization and enhanced production of prodigiosin from the spoiled coconut, Appl. Biochem. Biotechnol. 166 (2012) 187–196.
[5] A. Khanafari, M.M. Assadi, F.A. Fakhr, Review of prodigiosin, pigmentation in *Serratia marcescens*, Online J. Biol. Sci. 6 (2006) 1–13.
[6] A. Mortellaro, S. Songia, P. Gnocchi, M. Ferrari, C. Fornasiero, R. D'Alessio, A. Isetta, F. Colotta, J. Golay, New immunosuppressive drug PNU156804 Blocks IL-2-dependent proliferation and NF-κB and AP-1 activation, J. Immunol. (1999) 7102–7109.
[7] A.K. Harris, N.R. Williamson, H. Slater, A. Cox, S. Abbasi, I. Foulds, H.T. Simonsen, F.J. Leeper, G.P. Salmond, The *Serratia* gene cluster encoding biosynthesis of the red antibiotic, prodigiosin, shows species- and strain-dependent genome context variation, Microbiology 150 (2004) 3547–3560.
[8] S.R. Chawrai, N.R. Williamson, G.P.C. Salmond, F.J. Leeper, Chemoenzymatic synthesis of prodigiosin analogues – exploring the substrate specificity of PigC, Chem. Commun. (2008) 1862–1864.
[9] P.C. Fineran, H. Slater, L. Everson, K. Hughes, G.P.C. Salmond, Biosynthesis of tripyrrole and b-lactam secondary metabolites in *Serratia*: integration of quorum sensing with multiple new regulatory components in the control of prodigiosin and carbapenem antibiotic production, Mol. Microbiol. 56 (2005) 1495–1517.
[10] N.R. Williamson, H.T. Simonsen, R.A. Ahmed, G. Goldet, H. Slater, L. Woodley, F.J. Leeper, G.P. Salmond, Biosynthesis of the red antibiotic, prodigiosin, in *Serratia*: identification of a novel 2-methyl-3-n-amyl-pyrrole (MAP) assembly pathway, definition of the terminal condensing enzyme, and implications for undecylprodigiosin biosynthesis in *Streptomyces*, Mol. Microbiol. 56 (2005) 971–989.
[11] M.S. Humble, K.E. Cassimjee, M. Hakansson, Y.R. Kimbung, B. Walse, V. Abedi, H.J. Federsel, P. Berglund, D.T. Logan, Crystal structures of the *Chromobacterium violaceum* omega-transaminase reveal major structural rearrangements upon binding of coenzyme PLP, FEBS J. 279 (2012) 779–792.
[12] C.D. Chen, C.H. Lin, P. Chuankhayan, Y.C. Huang, Y.C. Hsieh, T.F. Huang, H.H. Guan, M.Y. Liu, W.C. Chang, C.J. Chen, Crystal structures of complexes of the branched-chain aminotransferase from *Deinococcus radiodurans* with alpha-ketoisocaproate and L-glutamate suggest the radiation resistance of this enzyme for catalysis, J. Bacteriol. 194 (2012) 6206–6216.
[13] P.K. Mehta, T.I. Hale, P. Christen, Aminotransferases: demonstration of homology and division into evolutionary subgroups, Eur. J. Biochem. 214 (1993) 549–561.
[14] S. Liu, T. Ran, X. Shen, L. Xu, W. Wang, D. Xu, Expression, crystallization and preliminary crystallographic data analysis of PigF, an O-methyltransferase from the prodigiosin-synthetic pathway in *Serratia*, Acta Crystallogr., Sect. F: Struct. Biol. Cryst. Commun. 68 (2012) 898–901.
[15] W. Kabsch, Xds, Acta Crystallogr. D Biol. Crystallogr. 66 (2010) 125–132.
[16] F. Long, A.A. Vagin, P. Young, G.N. Murshudov, BALBES: a molecular-replacement pipeline, Acta Crystallogr. D Biol. Crystallogr. 64 (2008) 125–132.
[17] P. Emsley, K. Cowtan, Coot: model-building tools for molecular graphics, Acta Crystallogr. D Biol. Crystallogr. 60 (2004) 2126–2132.
[18] G.N. Murshudov, A.A. Vagin, E.J. Dodson, Refinement of macromolecular structures by the maximum-likelihood method, Acta Crystallogr. D Biol. Crystallogr. 53 (1997) 240–255.
[19] W.L. DeLano, The PYMOL Molecular Graphics System, Delano Scientific LLC, San Carlos, CA, 2002.
[20] L. Holm, P. Rosenstrom, Dali server: conservation mapping in 3D, Nucleic Acids Res. 38 (2010) W545–W549.
[21] B.W. Shen, M. Hennig, E. Hohenester, J.N. Jansonius, T. Schirmer, Crystal structure of human recombinant ornithine aminotransferase, J. Mol. Biol. 277 (1998) 81–102.
[22] W. Liu, P.E. Peterson, R.J. Carter, X. Zhou, J.A. Langston, A.J. Fisher, M.D. Toney, Crystal structures of unbound and aminooxyacetate-bound *Escherichia coli* gamma-aminobutyrate aminotransferase, Biochemistry 43 (2004) 10896–10905.
[23] J. Newman, S. Seabrook, R. Surjadi, C.C. Williams, D. Lucent, M. Wilding, C. Scott, T.S. Peat, Determination of the structure of the catabolic succinylornithine transaminase (AstC) from *Escherichia coli*, PLoS ONE 8 (2013) 1–11.
[24] V.N. Malashkevich, P. Strop, J.W. Keller, J.N. Jansonius, M.D. Toney, Crystal structures of dialkylglycine decarboxylase inhibitor complexes, J. Mol. Biol. 294 (1999) 193–200.
[25] M. Hennig, B. Grimm, R. Contestabile, R.A. John, J.N. Jansonius, Crystal structure of glutamate-1-semialdehyde aminomutase: an alpha2-dimeric vitamin B6-dependent enzyme with asymmetry in structure and active site reactivity, Proc. Natl. Acad. Sci. U.S.A. 94 (1997) 4866–4871.